Dosimetric accuracy of a deterministic radiation transport based ^{192}Ir brachytherapy treatment planning system. Part III. Comparison to Monte Carlo simulation in voxelized anatomical computational models

K. Zourari,[a] E. Pantelis, and A. Moutsatsos
Medical Physics Laboratory, Medical School, University of Athens, 75 Mikras Asias, 115 27 Athens, Greece

L. Sakelliou
Department of Physics, Nuclear and Particle Physics Section, University of Athens, Ilisia, 157 71 Athens, Greece

E. Georgiou, P. Karaiskos, and P. Papagiannis[b]
Medical Physics Laboratory, Medical School, University of Athens, 75 Mikras Asias, 115 27 Athens, Greece

(Received 26 July 2012; revised 15 November 2012; accepted for publication 16 November 2012; published 18 December 2012)

Purpose: To compare TG43-based and Acuros deterministic radiation transport-based calculations of the BrachyVision treatment planning system (TPS) with corresponding Monte Carlo (MC) simulation results in heterogeneous patient geometries, in order to validate Acuros and quantify the accuracy improvement it marks relative to TG43.
Methods: Dosimetric comparisons in the form of isodose lines, percentage dose difference maps, and dose volume histogram results were performed for two voxelized mathematical models resembling an esophageal and a breast brachytherapy patient, as well as an actual breast brachytherapy patient model. The mathematical models were converted to digital imaging and communications in medicine (DICOM) image series for input to the TPS. The MCNP5 v.1.40 general-purpose simulation code input files for each model were prepared using information derived from the corresponding DICOM RT exports from the TPS.
Results: Comparisons of MC and TG43 results in all models showed significant differences, as reported previously in the literature and expected from the inability of the TG43 based algorithm to account for heterogeneities and model specific scatter conditions. A close agreement was observed between MC and Acuros results in all models except for a limited number of points that lay in the penumbra of perfectly shaped structures in the esophageal model, or at distances very close to the catheters in all models.
Conclusions: Acuros marks a significant dosimetry improvement relative to TG43. The assessment of the clinical significance of this accuracy improvement requires further work. Mathematical patient equivalent models and models prepared from actual patient CT series are useful complementary tools in the methodology outlined in this series of works for the benchmarking of any advanced dose calculation algorithm beyond TG43. © *2013 American Association of Physicists in Medicine*. [http://dx.doi.org/10.1118/1.4770275]

Key words: brachytherapy, ^{192}Ir, treatment planning, Monte Carlo, Acuros

I. INTRODUCTION

A treatment planning system (TPS) for ^{192}Ir brachytherapy under the commercial name BrachyVision (BV, Varian Medical Systems, Inc., Palo Alto, CA), incorporating a grid based Boltzmann equation solver (ACUROS, Transpire, Inc., Gig Harbor, WA) as an option to account for the dosimetric effects of material heterogeneities and radiation scatter conditions, received FDA approval and CE marking in 2009.[1]

A series of studies were designed for the independent dosimetric verification of this deterministic radiation transport based TPS approach through results comparison to reference dose distributions obtained using Monte Carlo simulation (MC) and experiment, as well as the evaluation of its impact to clinical practice through results comparison to the current standard for brachytherapy dosimetry based on the TG43 formalism. Previous studies discussed findings for single source dosimetry[2] and a multiple source dwell position plan employing a shielded applicator[3] in bounded geometries composed of homogeneous water. While societal recommendations for brachytherapy dosimetry beyond the TG43 have been published recently[4] and results on its clinical impact are becoming available without comparison to reference dose distributions,[5,6] this last addition to the aforementioned series reports on the benchmarking of BV-Acuros dosimetry in heterogeneous patient geometries using different voxelized anatomical computational models.

II. MATERIALS AND METHODS

II.A. TPS calculations

Two mathematical equation-based, stylized models and one computed tomography (CT) image-based tomographic model were used for the purposes of this work.

Details of the mathematical models simulating the anatomy of the thorax of a male and the breast of a female patient (including geometry, dimensions, and the organs or tissues considered) have been presented in previous studies in the literature[7,8] [see also Figs. 1(a) and 2(a)]. In order to facilitate their import to the TPS (BrachyVision v. 8.8), each mathematical model was voxelized through its conversion to a series of contiguous CT images in digital imaging and communications in medicine (DICOM) format. Hounsfield Units (HUs) were assigned following the inverse of the TPS procedure for material mapping. Each material was assigned the nominal density assumed by the TPS (see Table I) and corresponding HUs were derived by applying the TPS calibration curve. Details of the voxelized thoracic and breast mathematical models were as follows: 34 contiguous 16-bit grayscale resolution images of 5 mm slice thickness and 1.25 mm in-plane spatial resolution (320 mm FOV, 256 matrix); and 50 contiguous 16-bit grayscale images of 2 mm slice thickness and 0.5859 mm in-plane spatial resolution (150 mm FOV, 256 matrix), respectively. The two CT image series were imported to the TPS and volumes of interest (VOIs) were delineated using the TPS-embedded tools. For the thoracic model a brachytherapy plan resembling an esophageal treatment was created by employing 13 dwell positions of the VS2000 ^{192}Ir HDR source[9] in a plastic catheter, with a spacing of 5 mm and dwell times optimized to deliver a prescribed dose of 10 Gy at a distance of 0.5 cm from the catheter longitudinal axis. For the breast model, a planning target volume (PTV) was arbitrarily defined and a brachytherapy plan resembling an interstitial breast treatment was created using 10 plastic catheters and 39 VS2000 source dwell positions. A total dose of 32 Gy was prescribed at the 100% isodose line encompassing the PTV.

While mathematical models serve as test cases of user defined complexity for evaluating the performance of dose calculation algorithms, the endpoint is comparison for actual patient plans. The CT image series of an actual breast brachytherapy patient (32 contiguous 12-bit grayscale images of 3 mm slice thickness and 0.7168 mm in-plane spatial resolution, 367 mm FOV, 512 matrix) were therefore also used in this work as an image based patient model. CT images of the left breast of a patient were imported to the TPS and VOIs were delineated using the TPS-embedded tools. The 14 plastic catheters included in the image series were reconstructed and a brachytherapy treatment plan was created using 30 VS2000 source dwell positions. A total dose of 32 Gy was prescribed at the 100% isodose line encompassing the PTV.

The treatment plans for all three computational models were configured using the TG43 algorithm. Dosimetric calculations for the treatment plans were performed using both the TG43 and grid based Boltzmann solver options of the TPS (to be referred to in the following as BV-TG43 and BV-Acuros, respectively). In the latter case, the dose calculation and output grid extent was user defined. BV-Acuros automatically set the model region to be used as the input grid for calculations which is 10 cm larger than the output grid in each dimension to account for backscatter, unless the model boundary is reached. Plan details, delineated VOIs, reconstructed catheters and calculated dose matrices from all plans were exported in DICOM RT format. The spatial resolution of the RT dose object file was $1 \times 1 \times 1$ mm^3. All subsequent data manipulation for comparisons to corresponding MC results was conducted external to the TPS using custom made software routines.

II.B. Monte Carlo simulation

The MCNP5 v.1.40 (Ref. 10) general purpose MC code was used to obtain reference dose distributions for comparison with corresponding TPS results. Simulation models were prepared from the CT DICOM image series of the computational models imported to the TPS, using the capability of the employed MC code to define rectangular lattice geometries.[10]

Material properties were defined using a procedure identical to that of the TPS. HUs were converted to mass density using the TPS calibration curve. Seven material types were assigned on a voxel-by-voxel basis using the calculated density and the TPS table correlating density ranges to given materials (see Table I). Material elemental compositions were then assigned using the same source of data employed by the TPS.[11] In view of memory limitations for the patient breast model, images were down-sampled using a box interpolation kernel (pixel size was doubled to 1.4336 mm) and the density range corresponding to a given material was collapsed to its nominal density value (0.26 g cm^{-3}, see Table I). Test MC simulations were performed and verified that this does not affect the comparison between MC and BV-Acuros results. In example, the average lung density in the CT data is 0.32 g cm^{-3} and percentage dose differences between simulations of an ^{192}Ir point source centered in a sphere of lung tissue with density equal to the maximum and minimum values are under 2%. The MC simulation input files for each model were prepared using information derived from the corresponding DICOM RT export from the TPS (dwell positions, dwell times, total irradiation time and air kerma strength from RT plan, catheter coordinates from RT structures set, scoring grid geometry from RT dose). The VS2000 brachytherapy source was modeled as in a previous work[2] and a separate simulation was performed for each dwell position to preclude intersource attenuation that does not occur in clinical practice using remote afterloaders. Results were combined after weighting by the corresponding ratio of dwell time to the total irradiation time. In contrast to source dwell positions, the direction of the longitudinal source axis in them is not information available in RT plan and it was therefore deduced from the coordinates of two catheter points closely encompassing each dwell position.

Simulations were performed using the MCPLIB04 (Ref. 12) cross section data library and the ^{192}Ir photon spectrum from Glasgow and Dillman[13] considering only the penetrating part (i.e., photon energies greater than 11.3 keV). The

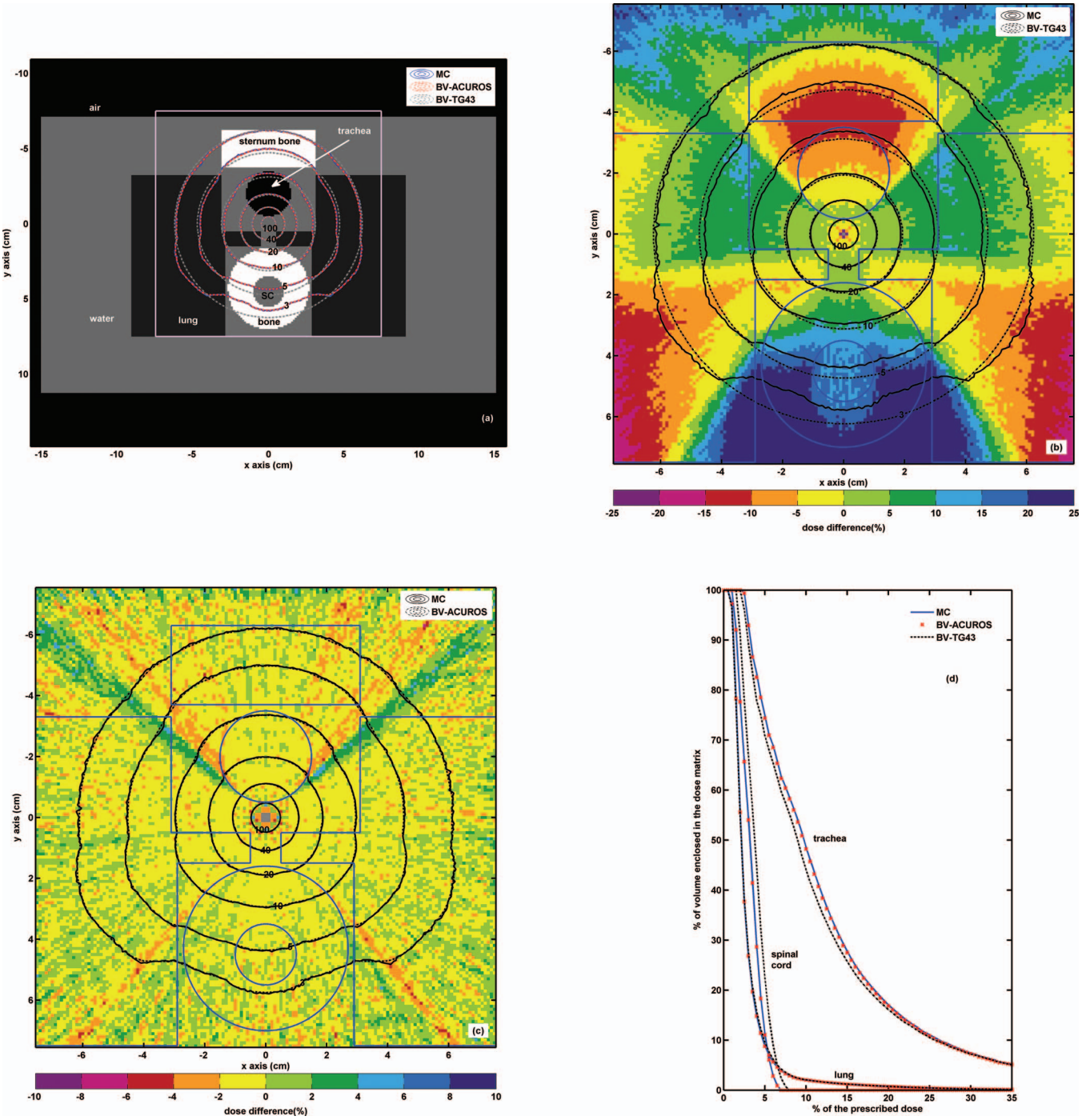

FIG. 1. (a) The central image of the voxelized mathematical thoracic model including lungs, spine, spinal cord, trachea, and sternum structures. BV-TG43, BV-ACUROS, and MC dose calculation results for the same esophagus brachytherapy plan are presented in the form of percentage isodose lines within the extent of the dose calculation grid. (b) A colormap representation of the spatial distribution of percentage differences between BV-TG43 and MC results ($\frac{D_{\text{BV-TG}_{43}}}{D_{\text{MC}}} - 1$) on the plane presented in (a). (c) A colormap representation of the spatial distribution of percentage differences between BV-Acuros and MC results ($\frac{D_{\text{BV-ACUROS}}}{D_{\text{MC}}} - 1$) on the plane presented in (a). (d) Cumulative DVH results for the lungs, spinal cord, and trachea OARs derived from the 3D dose distributions calculated using BV-TG43, BV-ACUROS, and MC.

relative uncertainty associated with cross section data is 2%.[14] Although contemporary data available for the ^{192}Ir photon spectrum are expected to be of improved accuracy relative to that in Glasgow and Dillman,[13] the latter were also used for the calculation of the VS2000 source TG43 dosimetric parameters employed by the TPS.[9] Besides, the contribution of uncertainty in the photon energy spectrum is negligible, and the relative uncertainty in photon yields cancels out for dose ratios such as those presented in this work.[14]

With the clinical availability of dose calculation methods beyond the TG43 assumptions, dose can be specified either in tissue or in water and the question of dose specification

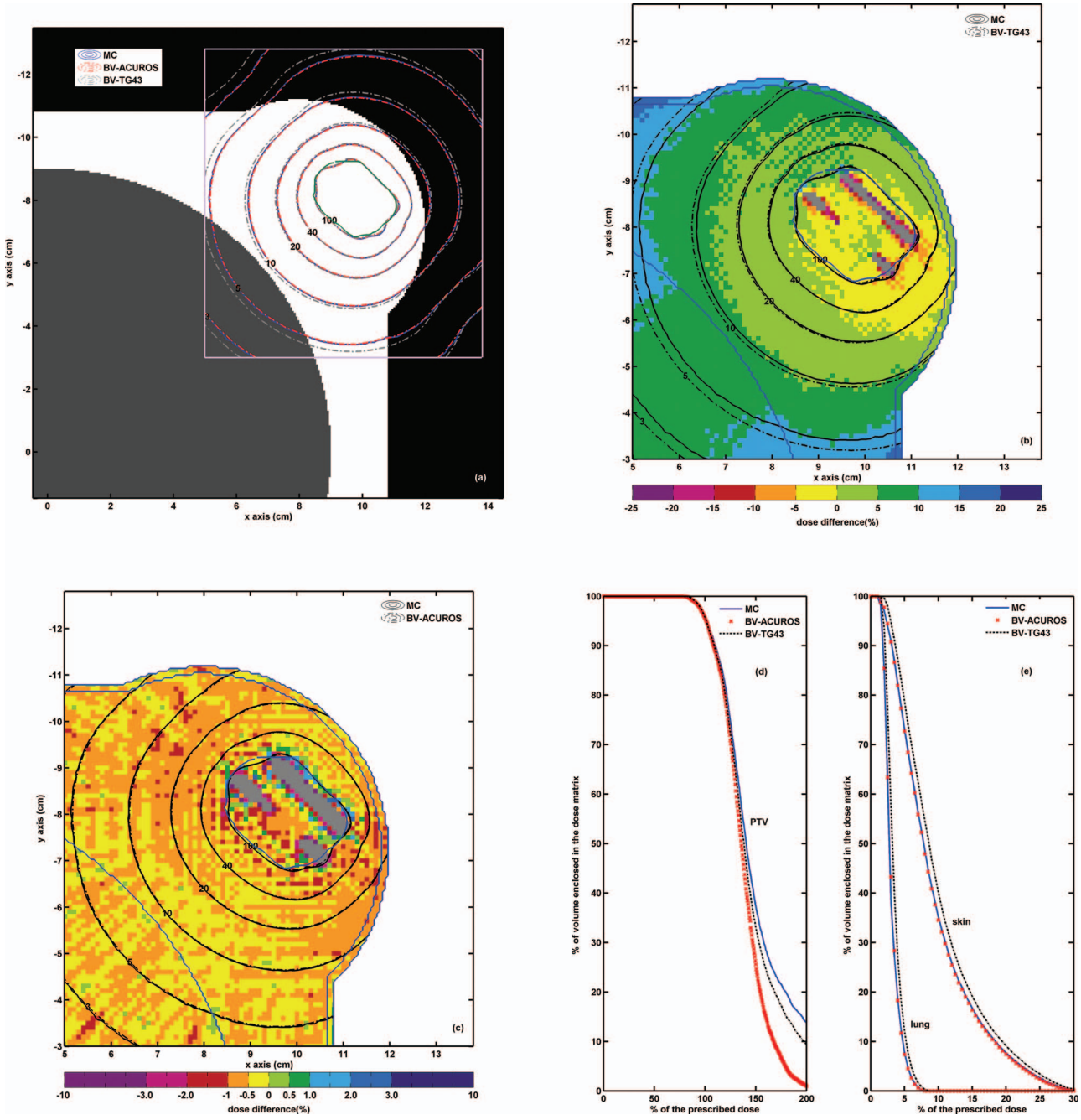

FIG. 2. (a) The central image of the voxelized mathematical breast model with BV-TG43, BV-ACUROS, and MC dose calculation results for the same breast brachytherapy plan presented in the form of percentage isodose lines within the extent of the dose calculation grid. (b) A colormap representation of the spatial distribution of percentage differences between BV-TG43 and MC results ($\frac{D_{\text{BV-TG}_{43}}}{D_{\text{MC}}} - 1$) on the plane presented in (a). (c) A colormap representation of the spatial distribution of percentage differences between BV-Acuros and MC results ($\frac{D_{\text{BV-ACUROS}}}{D_{\text{MC}}} - 1$) on the plane presented in (a). (d) Cumulative DVH results for the PTV derived from the 3D dose distributions calculated using BV-TG43, BV-ACUROS and MC. (e) Same as (d) for the skin and lung OARs.

medium has been recently linked to microdosimetric considerations of correlating the dose distribution to biologically relevant targets.[4] Since the TPS studied herein reports water collision kerma (in water in the case of BV-TG43 or in the heterogeneous model geometry in the case of BV-Acuros), secondary electron transport was not simulated in this work and water collision kerma was scored using the *FMESH4 tally with a resolution of $1 \times 1 \times 1$ mm^3 superimposed over the simulated model geometry. The specific tally calculates the track length estimate of the energy fluence averaged over a mesh cell in units of MeV cm^{-2} per starting photon, which was converted to MeV g^{-1} per starting photon using water mass energy absorption coefficients taken from NIST (Ref. 15) in the input files along with a dose energy and function card.

A different number of photon histories per source dwell position were simulated for each computational model. The estimated relative error at the 1σ level, as obtained using error

TABLE I. Materials included in the computational models of this work, along with the range of mass densities correlated by the TPS to these materials according to the BrachyVision-Acuros algorithm reference guide.

	Density (g cm^{-3})		
Material	Low	Nominal	High
Air (STP)	0.001	0.001205	0.1306
Lung	0.1306	0.26	0.605
Adipose tissue	0.605	0.92	0.985
Muscle, skeletal	0.985	1.05	1.075
Water[a]		1	
Cartilage	1.075	1.10	1.475
Bone	1.475	1.85	2.2275

[a]Comparison of BV-Acuros results for an ^{192}Ir point source centered in a homogeneous, 15 cm radius, sphere model of HU = 0 with corresponding MC simulation results in the same model comprising of either water or muscle tissue, suggests that the TPS assumes water material when HU is equal to zero (i.e., density equals unity).

propagation on the corresponding relative error values calculated by the MC code for each dwell position, is under 2% at all points in the mathematical esophageal model [1% in the region encompassed by the 3% isodose line, see Fig. 1(a)], under 1% at all points in the mathematical breast model [see Fig. 2(a)], and under 3% at all points in the real breast patient model [1% and 2% at short and intermediate distances from the PTV, respectively, see Fig. 3(a)]. Simulation results were converted to absorbed dose using the air kerma strength per starting photon value for the VS2000 source,[2] along with the information of source air kerma strength and total irradiation time of each treatment plan.

III. RESULTS

III.A. Dosimetry comparison in the voxelized mathematical models

Figure 1 presents results of the comparison between BV-TG43, BV-ACUROS, and MC dose calculations for the same esophagus brachytherapy plan in the voxelized mathematical thoracic model. In Fig. 1(a) results are presented in the form of percentage isodose lines superimposed on the central axial image of the model. In this figure, an overall good agreement can be seen for the relatively higher isodose lines lying close to the catheter. As distance from the catheter increases, however, BV-TG43 results deviate from the other two datasets as expected[7,8] due to the difference in the scatter and attenuation properties of the materials comprising the model geometry relative to water which is assumed in the calculation of the TG43 dosimetry data for the VS2000 source.[9]

Percentage differences between BV-TG43 and MC results are quantified in Fig. 1(b) on a pixel by pixel basis, and the former can be seen to overestimate the dose to the spinal cord by up to 20% and underestimate the dose to the sternum and the trachea by up to 15%. Percentage differences in the lungs are position dependent, reaching ±20%. In Fig. 1(c), where percentage differences between BV-Acuros and MC results are presented on a pixel by pixel basis on the same plane as in Fig. 1(b), an excellent agreement (±2%) can be seen for the majority of the presented points. In a limited number of points lying close to the directions defined by primary photon rays tangential to the spine and the trachea structures, however, BV-ACUROS results differ by up to 6% from corresponding MC results. This could be attributed to the ineffectiveness of the ray tracing algorithm employed by the TPS (Ref. 2) manifested only under extreme conditions such as the penumbra of a shield[3] or the ideally shaped spine and trachea structures of the model, as well as any difference in the discretization errors inherently involved in MC and BV-Acuros results.

Besides comparison in two dimensions, BV-TG43, BV-ACUROS, and MC results are also compared in the form of cumulative dose volume histograms (DVH) in Fig. 1(d). Agreement between all three datasets can be observed only for the case of the lung. This is in accordance with findings presented in Fig. 1(b) which suggest that the TG43 based dosimetric algorithm overestimates the delivered dose at the posterior part of lungs while underestimating it at the anterior part, and therefore a major fraction of these differences cancels out in terms of DVH values. Regarding the spinal cord and the trachea, it can be seen that the BV-TG43 calculated cumulative DVH is shifted toward higher and lower dose levels, respectively, relative to corresponding MC results, in agreement with results of Fig. 1(b). An excellent agreement between the BV-ACUROS and MC based calculated DVH results can be observed for all the organs at risk (OARs) presented in Fig. 1(d).

Figure 2(a) presents the comparison of BV-TG43, BV-ACUROS, and MC results for the same treatment plan in the voxelized mathematical breast model, in the form of percentage isodose lines superimposed on the central axial image of the model. While a good agreement can be observed between BV-ACUROS and MC results, TG43 results present an increasing dose overestimation relative to the other two datasets with increasing distance from the PTV. This dose overestimation is further quantified in Fig. 2(b) where percentage differences between BV-TG43 and MC results are presented on a pixel by pixel basis. In this figure, it can be seen that due to the combined effect of the lung heterogeneity and the finite patient dimensions, BV-TG43 significantly overestimates the dose distribution in agreement with previous findings in the literature.[8] Apart from this effect, a BV-TG43 dose underestimation greater than 25% is observed at points lying within the volume of the catheters (these points were not excluded from either dataset). A significant dose underestimation relative to MC results is also observed at points close to the sources probably due to the extrapolation algorithm employed by the TPS for points outside its input data grid. A slight dose underestimation is also observed in the positive x side of the PTV that is attributed to the different source drive wire length assumed in the simulations of this work[2] (1 mm) and the simulations for the data used as input to the TPS for TG43 based dose calculations[9] (15 cm).[16]

In Fig. 2(c), where percentage differences between BV-Acuros and MC results are presented on a pixel by pixel basis on the same plane as in Fig. 2(b), it can be seen that BV-Acuros succeeds in accounting for the lung heterogeneity and

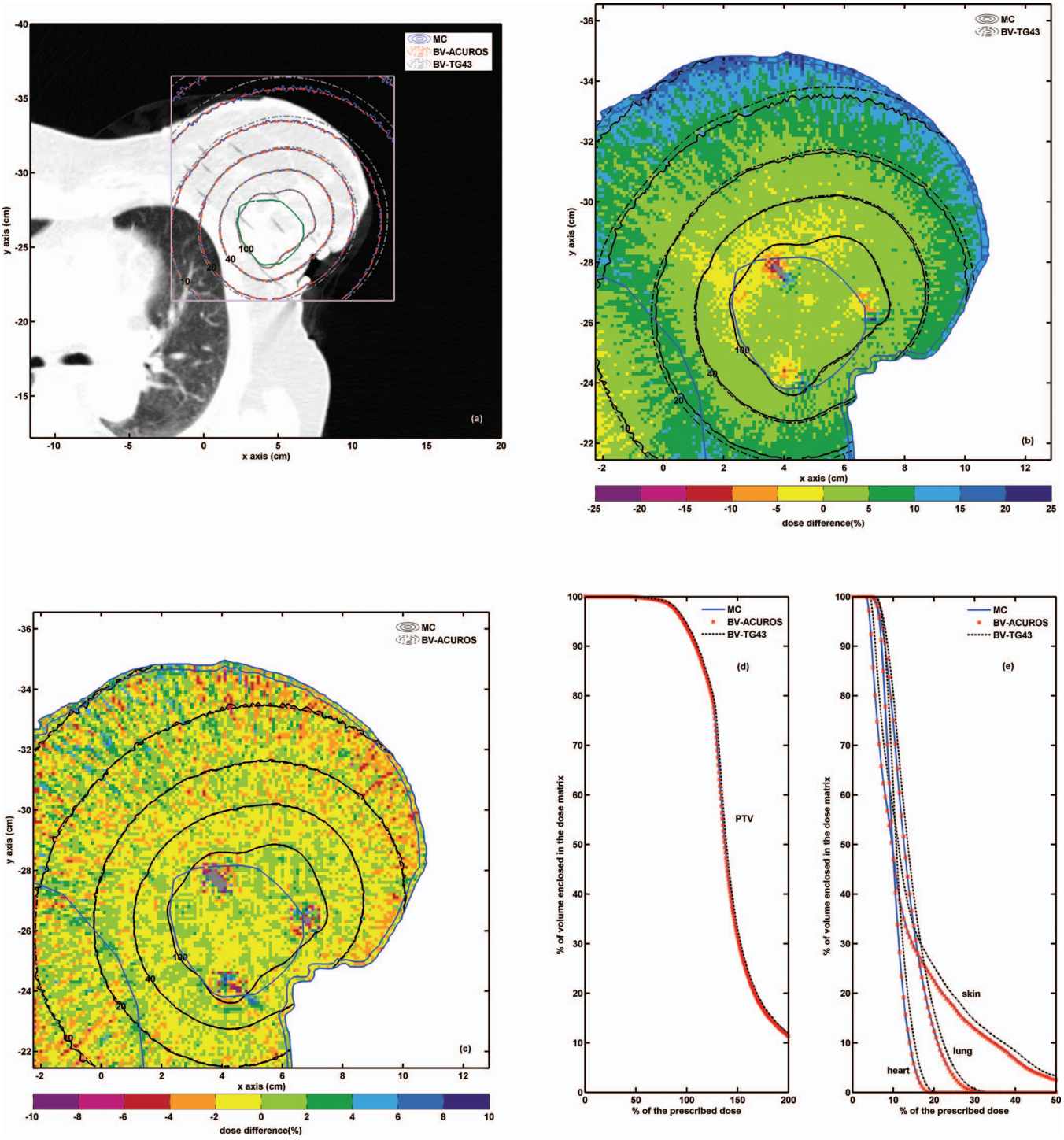

FIG. 3. (a) The central image of the breast patient computational model with BV-TG43, BV-ACUROS, and MC dose calculation results for the same breast brachytherapy plan presented in the form of percentage isodose lines within the extent of the dose calculation grid. (b) A colormap representation of the spatial distribution of percentage differences between BV-TG43 and MC results ($\frac{D_{\text{BV-TG}_{43}}}{D_{\text{MC}}} - 1$) on the plane presented in (a). (c) A colormap representation of the spatial distribution of percentage differences between BV-Acuros and MC results ($\frac{D_{\text{BV-ACUROS}}}{D_{\text{MC}}} - 1$) on the plane presented in (a). (d) Cumulative DVH results for the PTV derived from the 3D dose distributions calculated using BV-TG43, BV-ACUROS, and MC. (e) Same as (d) for the skin, lung, and heart OARs.

the geometry specific scatter conditions since agreement with MC results within $\pm 1\%$ is observed for the majority of points. Significant differences are only observed within the catheters (these points were not excluded from either dataset) as well as points close to the sources, probably, due to an inefficiency of the BV-Acuros ray tracing algorithm to predict the steep dose gradient close to the sources.

Cumulative DVH results derived from the dose distributions calculated using BV-TG43, BV-ACUROS, and MC for the same plan in the same breast model are presented in

Fig. 2(d). For the PTV, good agreement is observed for low percentage dose values; PTV coverage is comparable for all three datasets, and the same applies for the conformity index (defined as the ratio of reference isodose volume to target volume and found equal to: 0.960, 0.957, and 0.956 for MC, BV-TG43, and BV-Acuros, respectively). Agreement between the three datasets deteriorates as percentage dose increases, and significant differences between DVH results are observed at increased percentage dose levels that are also reflected on corresponding dose homogeneity index results [defined as $(V_{100\%}-V_{150\%})/V_{100\%}$ and found equal to: 0.642, 0.680, and 0.747 for MC, BV-TG43, and BV-Acuros, respectively]. These differences come from differences between the corresponding dose distributions discussed above at points inside or close to the catheters, and are therefore artificial to a large degree in view of the large fraction of the PTV corresponding to points inside the catheters for the small PTV volume studied (7.25 cm^3). For the lung and the skin OARs, BV-TG43 results in Fig. 2(d) can be seen to overestimate the DVHs relative to corresponding BV-Acuros and MC results which are in close agreement.

III.B. Dosimetry comparison in the patient model

Figure 3(a) presents the comparison of BV-TG43, BV-ACUROS, and MC results for the same treatment plan in the breast patient computational model, in the form of percentage isodose lines superimposed on the central axial image of the model. Similar to results in the voxelized mathematical breast model, a close agreement is observed between all three datasets close to the PTV. As distance from the PTV increases, BV-TG43 results overestimate the dose distribution. This dose overestimation is more evidently shown in Fig. 3(b) where percentage dose differences up to 10% in the lung and 20% in the breast skin are observed between of BV-TG43 and MC results. In accordance with findings discussed above for the mathematical breast model, a BV-TG43 dose underestimation is observed within or close to the catheters, as well as in the drive wire side of the PTV.

In Fig. 3(c), where percentage differences between BV-Acuros and MC results are presented on a pixel by pixel basis on the same plane as in Fig. 2(b), it can be seen that BV-Acuros provides dose calculation accuracy comparable to MC since agreement within ±2% is observed for the majority of points. As with the case of the mathematical breast model, significant differences are only observed within or close to the catheters. In contrast to results in Fig. 2(d), however, these differences do not significantly affect PTV DVH results due to the relatively larger PTV volume (45.86 cm^3). This is shown in Fig. 3(d) where cumulative DVH results derived from the dose distributions calculated using BV-TG43, BV-ACUROS, and MC are in close agreement for the PTV, with a minor underestimation observed for BV-Acuros at relatively increased percentage dose values. PTV coverage is comparable for all three datasets, and the same applies for the conformity index (0.901, 0.900, and 0.901 for MC, BV-TG43, and BV-Acuros, respectively) and the dose homogeneity index (0.673, 0.669, 0.676 for MC, BV-TG43, and BV-Acuros, respectively). BV-Acuros and MC DVH results for the OARs in Fig. 3(d) are in close agreement, with a slight overestimation discernible for BV-TG43 results.

IV. DISCUSSION

Ample literature exists that presents data similar to the comparison between MC and BV-TG43 results performed in this work to quantify the accuracy improvement achieved by BV-Acuros.

In an early study using TLD and film measurements in phantoms as well as *in vivo*, Mangold *et al.*[17] reported an average dose overestimation of 14% at the tissue-air interface in an experimental quality control study of PDR ^{192}Ir interstitial breast brachytherapy performed using TG43-based treatment planning.

Anagnostopoulos *et al.*[7] and Pantelis *et al.*[8] compared MCNPX simulation results to TG43-equivalent dose calculations in the original studies introducing the mathematical computational models resembling an esophageal and an interstitial breast brachytherapy patient that were also used in this work. Their results are in agreement with the comparison of MC and BV-TG43 presented in this work besides methodological differences including the use of a different ^{192}Ir source and plan, tissue elemental compositions adopted from different sources [ICRU Report 44 (Ref. 18) versus ICRP Report 23 (Ref. 11) in this work], different cross section libraries (MCPLIB02 versus MCPLIB04 used in this work), the fact that tissue kerma in tissue was scored in the original studies, and the voxelization of the mathematical computational models in this work.

Within the context of introducing an analytical scatter correction technique as an alternative to TG43 based calculations, Poon and Verhaegen[19] compared PTRAN CT MC (Ref. 20) simulations in the CT-based geometries of 18 multicatheter breast brachytherapy patients to TG43 based dose calculations, taking into account four tissue types (lung, adipose, soft tissue, and rib bone) with elemental compositions according to the ICRU Report 44.[18] Their results, presented in the form of isodose lines and DVHs for an indicative patient and tabulated DVH statistics for the patient cohort, are compatible with corresponding results of this work showing a TG43 dose overestimation of skin, heart, and lung. On average, all presented DVH statistics were overestimated by TG43 (i.e., 5%, 2%, and 5% for skin, heart, and lung $D_{0.1cc}$, respectively) with considerable variation between patients.[19]

In a subsequent study[21] proposing a CT-based analytical dose calculation method for HDR ^{192}Ir brachytherapy, the same authors compared PTRAN CT MC (Ref. 20) simulations and TG43 calculations in the CT-based geometry of an esophageal brachytherapy patient and reported results similar to those of Anagnostopoulos *et al.*[7] and this work. The same comparison in the CT-based geometry of an intracavitary breast brachytherapy case with a balloon applicator filled with iodine contrast solution, showed that TG43 overestimated dose to the target, skin, and ipsilateral lung by more than 5%.

The comprehensive experimental study of Raffi *et al.*[22] also reported a TG43-based TPS skin dose overestimation in intracavitary breast brachytherapy employing contrast filled balloon applicators. While TLD measurements, MCNP5 simulation, and TG43-based treatment planning were found in excellent agreement in phantoms simulating TPS assumptions, the TG43-based results were shown to overestimate exit skin dose to water 9%–15% for phantom setups simulating treatment conditions and by 16%, on average, for a group of 59 patients, with a considerable variation between fractions and patients (TLD and TPS difference ranged from −13% to 47%).

The only study reporting findings that are not compatible, at least qualitatively, with the results of the comparison between MC and BV-TG43 presented in this work is that of Mille *et al.*[23] This study was based on MCNPX simulations in a virtual balloon breast brachytherapy patient prepared from voxelizing the RPI-adult female computational model.[24] A comparison between MCNPX results in the inhomogeneous model and the same model with all the tissues set to water was included for a point ^{192}Ir source centered in a balloon modeled as a sphere of water. The latter results are equivalent to TG43 based dose calculations taking, however, into account the finite patient dimensions and, therefore, skin dose was found comparable in the inhomogeneous and water computational models.[23] Isodose line comparison, average dose results, and DVH results for the ipsilateral lung, however, all suggest that the dose to the lung was found greater in the inhomogeneous model (i.e., 640 cGy average organ dose relative to 593 cGy in the water model) in contrast to results presented in this and previous studies.[8,19,21] Although some influence from the scatter conditions configured by the finite patient dimensions to the dose to the lung cannot be ruled out, it is not clear whether these findings are justified by the source-organ geometry and other assumptions in the study of Mille *et al.*,[23] or associated with the methods used for tallying and the tally conversion to dose.

The results discussed above support that, on average, TG43 based dosimetry overestimates dose to the skin, heart, and lung OARs with a percentage dose difference between TG43 and reference dose distributions that depend more on patient and treatment specific geometric parameters than on the details of the methodology used to calculate the reference dose distributions.

Besides differences in their aim and methods, the studies discussed above seek to quantify the inaccuracies of TG43 based dosimetry either experimentally or through the use of computational models that are as close to reality as possible with regard to geometry, tissue density, and tissue elemental composition. This work is fundamentally different, focusing to the validation of BV-Acuros dosimetry. Since BV-Acuros was the first dose calculation engine beyond TG43 that is clinically available, meticulous work was done to configure MC simulations so that their input is as close as possible to the input of BV-Acuros and ensure there is no bias in the comparison of their outputs. Whether the computational models included in this input are the most realistic that can be achieved or representative of individual or average patients is beyond the scope of this work. In this context, results of this work show that, when provided with the same input, BV-Acuros achieves accuracy comparable to MC except for a limited number of points lying in the penumbra of perfectly shaped structures that can only be met in mathematical computational models and points within the catheters or close to the source that are not clinically significant.

V. CONCLUSIONS

Dosimetric calculations were performed in voxelized anatomical computational models of heterogeneous patient geometries using Monte Carlo simulation as well as the TG43 and Acuros grid based Boltzmann solver options of the BrachyVision treatment planning system (abbreviated as BV-TG43 and BV-Acuros, respectively, in this work). Comparison of BV-TG43 and Monte Carlo results verified the shortcomings of the, otherwise robust and computationally nonintensive, TG43 formalism.[7,8,17,19,21,22] While the BV-Acuros dose calculation engine is not currently used for optimization and dose prescription, it was found to correctly account for heterogeneities and patient specific scatter conditions providing accuracy comparable to Monte Carlo simulation. The clinical significance of the improved accuracy offered by BV-Acuros remains to be evaluated in studies of site specific treatment plan cohorts.

Mathematically, patient equivalent models and models prepared from actual patient CT series proved complementary tools for testing the dosimetric accuracy of BV-Acuros; the former comprising an unambiguous means to define a test case for comparisons without bias from organ geometry and material properties delineation and the latter serving as an integral test of conditions met in actual clinical practice.

This work, combined with the previous two in the series,[2,3] forms a protocol of tests and methods useful for a thorough benchmarking of any advanced brachytherapy treatment planning system beyond TG43.

ACKNOWLEDGMENTS

This work was performed within the framework of a consultancy project appointed by Varian Medical Systems for the independent validation of a deterministic radiation transport based ^{192}Ir brachytherapy treatment planning system. This research has been cofinanced by the European Union (European Social Fund--ESF) and Greek national funds through the Operational Program "Education and Lifelong Learning" of the National Strategic Reference Framework (NSRF)—Research Funding Program: Heracleitus II. Investing in knowledge society through the European Social Fund.

[a]Electronic mail: kzourari@med.uoa.gr
[b]Author to whom correspondence should be addressed. Electronic mail: ppapagi@phys.uoa.gr

[1] M. J. Rivard, L. Beaulieu, and F. Mourtada, "Enhancements to commissioning techniques and quality assurance of brachytherapy treatment planning systems that use model-based dose calculation algorithms," Med. Phys. **37**, 2645–2658 (2010).

[2]K. Zourari, E. Pantelis, A. Moutsatsos, L. Petrokokkinos, P. Karaiskos, L. Sakelliou, E. Georgiou, and P. Papagiannis, "Dosimetric accuracy of a deterministic radiation transport based ^{192}Ir brachytherapy treatment planning system. Part I: Single sources and bounded homogeneous geometries," Med. Phys. **37**, 649–661 (2010).

[3]L. Petrokokkinos, K. Zourari, E. Pantelis, A. Moutsatsos, P. Karaiskos, L. Sakelliou, I. Seimenis, E. Georgiou, and P. Papagiannis, "Dosimetric accuracy of a deterministic radiation transport based ^{192}Ir brachytherapy treatment planning system. Part II: Monte Carlo and experimental verification of a multiple source dwell position plan employing a shielded applicator," Med. Phys. **38**, 1981–1992 (2011).

[4]L. Beaulieu, A. Carlsson Tedgren, J. F. Carrier, S. D. Davis, F. Mourtada, M. J. Rivard, R. M. Thomson, F. Verhaegen, T. A. Wareing, and J. F. Williamson, "Report of the Task Group 186 on model-based dose calculation methods in brachytherapy beyond the TG-43 formalism: Current status and recommendations for clinical implementation," Med. Phys. **39**, 6208–6236 (2012).

[5]D. E. Hyer, A. Sheybani, G. M. Jacobson, and Y. Kim, "The dosimetric impact of heterogeneity corrections in high-dose rate (192)Ir brachytherapy for cervical cancer: Investigation of both conventional Point-A and volume-optimized plans," Brachytherapy **11**, 515–520 (2012).

[6]J. K. Mikell, A. H. Klopp, G. M. Gonzalez, K. D. Kisling, M. J. Price, P. A. Berner, P. J. Eifel, and F. Mourtada, "Impact of heterogeneity-based dose calculation using a deterministic grid-based Boltzmann equation solver for intracavitary brachytherapy," Int. J. Radiat. Oncol., Biol., Phys. **83**, 417–422 (2012).

[7]G. Anagnostopoulos, D. Baltas, E. Pantelis, P. Papagiannis, and L. Sakelliou, "The effect of patient inhomogeneities in oesophageal ^{192}Ir HDR brachytherapy: A Monte Carlo and analytical dosimetry study," Phys. Med. Biol. **49**, 2675–2685 (2004).

[8]E. Pantelis, P. Papagiannis, P. Karaiskos, A. Angelopoulos, G. Anagnostopoulos, D. Baltas, N. Zamboglou, and L. Sakelliou, "The effect of finite patient dimensions and tissue inhomogeneities on dosimetry planning of ^{192}Ir HDR breast brachytherapy: A Monte Carlo dose verification study," Int. J. Radiat. Oncol., Biol., Phys. **61**, 1596–1602 (2005).

[9]A. Angelopoulos, P. Baras, L. Sakelliou, P. Karaiskos, and P. Sandilos, "Monte Carlo dosimetry of a new ^{192}Ir high dose rate brachytherapy source," Med. Phys. **27**, 2521–2527 (2000).

[10]E. T. Booth, "MCNP-A general Monte Carlo N-particle transport code, version 5," Report No. LA-UR-03-1987, 2003.

[11]ICRP, "Report of the task group on reference man," Ann. ICRP **23**, 1–480 (1975).

[12]M. C. White, "Photoatomic Data Library MCNPLIB04: A new photoatomic library based on data from ENDF/B-VI Release 8," Los Alamos National Laboratory Internal Memorandum X-5:MCW-020111, 2002.

[13]G. P. Glasgow and L. T. Dillman, "Specific gamma-ray constant and exposure rate constant of ^{192}Ir," Med. Phys. **6**, 49–52 (1979).

[14]D. C. Medich, M. A. Tries, and J. J. Munro II, "Monte Carlo characterization of an ytterbium-169 high dose rate brachytherapy source with analysis of statistical uncertainty," Med. Phys. **33**, 163–172 (2006).

[15]J. H. Hubbell and S. M. Seltzer, "Tables of X-Ray Mass Attenuation Coefficients and Mass Energy-Absorption Coefficients (version 1.4)." Available: http://physics.nist.gov/xaamdi. National Institute of Standards and Technology, Gaithersburg, MD. Originally published as NISTIR 5632, National Institute of Standards and Technology, Gaithersburg, MD (1995).

[16]J. K. Mikell and F. Mourtada, "Dosimetric impact of an ^{192}Ir brachytherapy source cable length modeled using a grid-based Boltzmann transport equation solver," Med. Phys. **37**, 4525–5148 (2010).

[17]C. A. Mangold, A. Rijnders, D. Georg, E. Van Limbergen, R. Potter, and D. Huyskens, "Quality control in interstitial brachytherapy of the breast using pulsed dose rate: Treatment planning and dose delivery with an Ir-192 afterloading system," Radiother. Oncol. **58**, 43–51 (2001).

[18]ICRU, Tissue Substitutes in Radiation Dosimetry and Measurement, ICRU Report 44, ICRU, Bethesda, MD, 1989.

[19]E. Poon and F. Verhaegen, "Development of a scatter correction technique and its application to HDR ^{192}Ir multicatheter breast brachytherapy," Med. Phys. **36**, 3703–3713 (2009).

[20]Y. Le, O. Chibani, D. Todor, J. Siebers, and J. F. Williamson, "An integrated CT-based Monte Carlo dose-evaluation system for brachytherapy and its application to permanent prostate implant postprocedure dosimetric analysis," Med. Phys. **32**, 2068 (2005).

[21]E. Poon and F. Verhaegen, "A CT-based analytical dose calculation method for HDR ^{192}Ir brachytherapy," Med. Phys. **36**, 3982–3994 (2009).

[22]J. A. Raffi, S. D. Davis, C. G. Hammer, J. A. Micka, K. A. Kunugi, J. E. Musgrove, J. W. Winston, T. J. Ricci-Ott, and L. De Werd, "Determination of exit skin dose for ^{192}Ir intracavitary accelerated partial breast irradiation with thermoluminescent dosimeters," Med. Phys. **37**, 2693–702 (2010).

[23]M. M. Mille, X. G. Xu, and M. J. Rivard, "Comparison of organ doses for patients undergoing balloon brachytherapy of the breast with HDR ^{192}Ir or electronic sources using Monte Carlo simulations in a heterogeneous human phantom," Med. Phys. **37**, 662–671 (2010).

[24]J. Zhang, Y. H. Na, P. F. Caracappa, and X. G. Xu, "RPI-AM and RPI-AF, a pair of mesh-based, size-adjustable adult male and female computational phantoms using ICRP-89 parameters and their calculations for organ doses from monoenergetic photon beams," Phys. Med. Biol. **54**, 5885–5908 (2009).